2011 31st International Conference on Distributed Computing Systems

Resource Allocation for Medium Grain Scalable Videos over Femtocell Cognitive Radio Networks

Donglin Hu and Shiwen Mao
Department of Electrical and Computer Engineering
Auburn University, Auburn, AL 36839-5201, USA
Email: dzh0003@auburn.edu, smao@ieee.org

***Abstract*—Femtocells are shown highly effective on improving network coverage and capacity by bringing base stations closer to mobile users. In this paper, we investigate the problem of streaming scalable videos in femtocell cognitive radio (CR) networks. This is a challenging problem due to the stringent QoS requirements of real-time videos and the new dimensions of network dynamics and uncertainties in CR networks. We develop a framework that captures the key design issues and trade-offs with a *stochastic programming* problem formulation. In the case of a single FBS, we develop an optimum-achieving distributed algorithm, which is shown also optimal for the case of multiple non-interfering FBS's. In the case of interfering FBS's, we develop a greedy algorithm that can compute near-optimal solutions, and prove a closed-form lower bound for its performance. The proposed algorithms are evaluated with simulations, and are shown to outperform two alternative schemes with considerable margins.**

I. Introduction

According to a recent study by Cisco, potential wireless data traffic is expected to increase by a factor of 66 from 2009 to 2013 [1]. Furthermore, almost 66 percent of the mobile data will be video by 2013, as driven by the availability of intelligent mobile devices and the compelling need for ubiquitous access to wireless multimedia content. Such drastic increase in wireless video traffic will significantly stress the capacity of existing and future wireless networks and will have far-reaching impacts on how future wireless networks are designed and operated.

Due to the use of open space as transmission medium, capacity of wireless networks are usually limited by interference. When a mobile user moves away from the base station, a considerably larger transmit power is needed to overcome attenuation, while causing interference to other users and deteriorating network capacity. To this end, femtocells provide an effective solution that brings base stations closer to mobile users. A femtocell usually has a size of (or even smaller than) a residential cellular network, with a *femto base station* (FBS) connected to the owner's broadband wireline network [2], [3]. The FBS serves approved subscribers when they are within the coverage. Among the many benefits, femtocells are shown effective on improving network coverage and capacity [2]. Due to the reduced distance of wireless links, transmit power can be greatly reduced, leading to prolonged battery life, improved signal-to-interference-plus-noise ratio (SINR), and better spatial reuse of spectrum.

Femtocells have received significant interest from the wireless industry. Many wireless operators have launched femtocell service recently, such as AT&T, Sprint, Verizon, and Vodafone. Although highly promising, several important problems should be addressed to fully harvest the high potential of femtocells, such as interference mitigation, resource allocation, synchronization, and QoS provisioning [2], [3]. It is also critical for the success of this technology to support important applications such as real-time video streaming in femtocell networks.

In this paper, we investigate the problem of video streaming in femtocell cognitive radio (CR) networks. We consider a femtocell network consisting of a *macro base station* (MBS) and multiple FBS's. The femtocell network is co-located with a primary network with multiple licensed channels. The idea is to exploit CR and dynamic spectrum access to utilize spectrum opportunities in the licensed channels for streaming videos [4]. Femtocell subscribers (or, CR users) and FBS's sense licensed channels, and determine which channel(s) and which base station (i.e., the MBS or an FBS) to use for delivering video packets based on sensing results. The objective is to maximize the capacity of the femtocell CR network on carrying real-time video data, while bounding the interference to primary users.

This is a challenging problem due to the stringent QoS requirements of real-time videos and, on the other hand, the new dimensions of network dynamics (i.e., channel availability) and uncertainties (i.e., spectrum sensing and errors) found in CR networks. It also involves a long list of design factors that necessitates cross-layer optimization, such as spectrum sensing and errors, dynamic spectrum access, interference modeling and primary user protection, channel allocation, and video performance, among others.

We adopt Scalable Video Coding (SVC) in our system. SVC encodes a video stream consisting of multiple substreams, subsets of which can be decoded to provide different quality levels for the reconstructed video [5]. Such scalability is very useful for video streaming systems, especially in CR networks, to accommodate heterogeneous channel availabilities and dynamic network conditions. We consider H.264/SVC medium grain scalable (MGS) videos, rather than Fine-Granularity-Scalability (FGS) videos. MGS can achieve better rate-distortion performance over FGS,

1063-6927/11 $26.00 © 2011 IEEE
DOI 10.1109/ICDCS.2011.18

although MGS only has Network Abstraction Layer (NAL) unit-based granularity [5].

The unique femtocell network architecture and the scalable video adopted in this paper allow us to develop a framework that captures the key design issues and tradeoffs, and to formulate a *stochastic programming* problem. It has been shown that the deployment of femtocells has a significant impact on the network performance [2]. In this paper, we examine three deployment scenarios. In the case of a single FBS, we apply the *dual decomposition* technique to develop a distributed algorithm that can compute the optimal solution to the formulated problem. In the case of multiple non-interfering FBS's, we show that the same distributed algorithm can be used to compute optimal solutions. In the case of multiple interfering FBS's, we develop a greedy algorithm that can compute near-optimal solutions, and prove a closed-form lower bound for its performance based on an *interference graph* model. The proposed algorithms are evaluated with simulations, and are shown to outperform two alternative schemes with considerable gains. We find the video quality is not very sensitive to sensing errors, since both types of errors are modeled in the optimization framework. We also find that it is not necessary to have a very large bandwidth for the MBS common channel, since the gain for additional MBS channel bandwidth diminishes as it gets large.

The remainder of this paper is organized as follows. The related work is discussed in Section II. The system model and preliminaries are given in Section III. We present the problem formulation and develop solution algorithms in Section IV. Simulation results are presented in Section V. Section VI concludes this paper.

II. Related Work

Femtocells have received considerable interest from both industry and academia. Comprehensive overviews of technical challenges, requirements, and some preliminary solutions to femtocell networks can be found in [2] and [3]. Since femtocells can use the same channels as conventional cellular networks, considerable research efforts were focused on interference analysis and mitigation [6]–[8], which is important for the success of this technology. In [6], a distributed utility-based SINR adaptation scheme at femtocells was proposed to alleviate cross-tier interference at the macrocell from co-channel femtocells. In [7], the authors proposed a fractional frequency reuse scheme to mitigate inter-femtocell interference. Co-channel interference analysis and cancellation were considered in [8].

The high potential of CRs has attracted significant interest from the wireless community [4], [9]. The mainstream CR research has been focused on spectrum sensing, dynamic spectrum access, and other networking-related issues. In a recent work [10], Jin and Li proposed to adopt CR and cooperative communications in femtocell WiMAX networks. A stochastic Lyapunov optimization-based framework was presented. The proposed resource management protocol is shown to be near-optimal with closed-form bounds.

The problem of video over CR networks has only been addressed in a few papers [11]–[15]. In [11], Shiang and van der Schaar presented a dynamic channel selection scheme for CR users to transmit videos over multiple channels. In [12], Ali and Yu considered transmitting a video stream over a CR link and provided a partially observable Markov decision process (POMDP) formulation and solution procedure. In [13], a distributed joint routing and spectrum sharing algorithm for video streaming applications over CR ad hoc networks is proposed and evaluated with simulations. In our prior work [15], we considered multicasting FGS videos in an infrastructure-based CR network. We presented effective greedy heuristic algorithms for scheduling video data, with proven optimality bound.

In this paper, we consider the challenging problem of real-time video streaming over femtocell CR networks, where a broad spectrum of design factors should be considered in addition to interference mitigation. The unique network architecture leads to a stochastic programming formulation, for which we develop an optimum-achieving distributed algorithm for non-interfering femtocells, and a greedy algorithm for interfering femtocells, along with a proven closed-form low bound.

III. System Model and Preliminaries

A. Spectrum and Network Model

We consider a spectrum consisting of $M+1$ channels, including one common, unlicensed channel (indexed as channel 0) and M licensed channels (indexed as channels 1 to M). The M licensed channels are allocated to a primary network serving primary users, and the common channel is exclusively used by all CR users. All the $M+1$ channels follow a synchronized time slot structure [4]. We assume the capacity of all licensed channels are identical as B_1 Mbps, while the capacity of the common channel is B_0 Mbps.

The channel states evolve independently, while the occupancy of each licensed channel follows a two-state discrete-time Markov process, as validated by several measurement studies [16], [17] and used in prior work [4], [18]. The network status in time slot t is denoted as $\vec{S}(t) = [S_1(t), S_2(t), \cdots, S_M(t)]$, where $S_m(t)$ is the status of channel m with either idle (when $S_m(t)=0$) or busy (when $S_m(t)=1$) states. Let P_m^{01} and P_m^{10} be the transition probability from state 0 to 1 and that from state 1 to 0 for channel m, respectively. The utilization of channel m with respect to primary user transmissions can be written as:

$$\eta_m = \lim_{T\to\infty} \frac{1}{T}\sum_{t=1}^{T} S_m(t) = P_m^{01} / \left[P_m^{01} + P_m^{10}\right]. \qquad (1)$$

The femtocell CR network is illustrated in Fig. 1. There is an MBS and N FBS's deployed in the area to serve

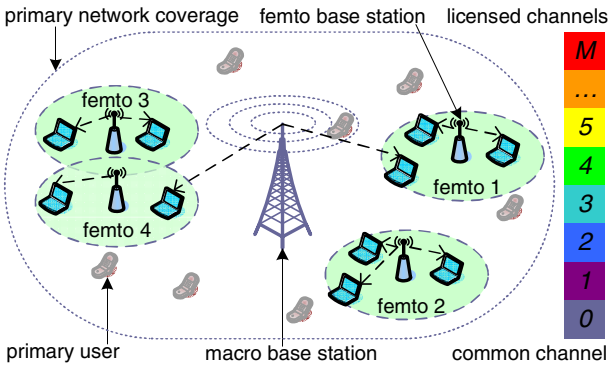

Figure 1. A femtocell CR network with one MBS and four FBS's.

CR users. The N FBS's are connected to the MBS (and the Internet) via broadband wireline connections. Due to advances in antenna technology, it is possible to equip multiple antennas at the base stations. The MBS has one antenna that is always tuned to the common channel. Each FBS is equipped with multiple antennas (e.g., M) and is able to sense multiple licensed channels at the beginning of each time slot. There are K_i CR users in femtocell i, $i = 1, 2, \cdots, N$, and $\sum_{i=1}^{N} K_i = K$. Each CR user has a software radio transceiver, which can be tuned to any of the M+1 channels. A CR user will either connect to a nearby FBS using one or more of the licensed channels or to the MBS via the common channel.

B. Spectrum Sensing

The femtocell CR network is within the coverage of the infrastructure-based primary network. Both FBS's and CR users sense the channels to identify spectrum opportunities in each time slot. Each time slot consists of (i) a *sensing phase*, when CR users and FBS's sense licensed channels, (ii) a *transmission phase*, when CR users and FBS's attempt to access licensed channels based on sensing results, and (iii) an *acknowledgment phase*, when CR receivers transmit acknowledgments to the sources. Each CR user chooses one channel to sense in a time slot, since it only has one transceiver. The sensing results will be shared among CR users and FBS's via the common channel.

We adopt a *hypothesis test* to detect channel availability. The null hypothesis H_0^m and the alternative hypothesis H_1^m are: $H_0^m :=$ {channel m is idle} and $H_1^m :=$ {channel m is busy}. For spectrum sensing, two kinds of detection errors may occur: (i) *false alarm*, an idle channel is considered busy and a spectrum opportunity will be wasted; (ii) *miss detection*, a busy channel is considered idle, which may lead to collision with primary users. Let ϵ_i^m and δ_i^m be the false alarm and miss detection probabilities of the i-th sensing result, respectively. We then have

$$\Pr\{\Theta_i^m = 1 | H_0^m\} = \epsilon_i^m \quad \text{and} \quad \Pr\{\Theta_i^m = 0 | H_1^m\} = \delta_i^m,$$

where Θ_i^m is the i-th sensing result on channel m. Given L sensing results on channel m, the conditional probability $P_m^A(\Theta_1^m, \cdots, \Theta_L^m)$ that channel m is available is

$$P_m^A(\vec{\Theta}_m) = P_m^A(\Theta_1^m, \cdots, \Theta_L^m) = \Pr\{H_0^m | \Theta_1^m, \cdots, \Theta_L^m\} = \left[1 + \frac{\eta_m}{1-\eta_m} \prod_{i=1}^{L} \frac{(\delta_i^m)^{1-\Theta_i^m}(1-\delta_i^m)^{\Theta_i^m}}{(\epsilon_i^m)^{\Theta_i^m}(1-\epsilon_i^m)^{1-\Theta_i^m}}\right]^{-1} \quad (2)$$

The availability of channel m, i.e., $P_m^A(\Theta_1^m, \cdots, \Theta_L^m)$, can be computed iteratively by decomposing (2) as follows.

$$P_m^A(\Theta_1^m) = \left[1 + \frac{\eta_m}{1-\eta_m} \times \frac{(\delta_1^m)^{1-\Theta_1^m}(1-\delta_1^m)^{\Theta_1^m}}{(\epsilon_1^m)^{\Theta_1^m}(1-\epsilon_1^m)^{1-\Theta_1^m}}\right]^{-1} \quad (3)$$

$$P_m^A(\Theta_1^m, \Theta_2^m, \cdots, \Theta_l^m) = \left\{1 + \left[\frac{1}{P_m^A(\Theta_1^m, \Theta_2^m, \cdots, \Theta_{l-1}^m)} - 1\right] \times \frac{(\delta_l^m)^{1-\Theta_l^m}(1-\delta_l^m)^{\Theta_l^m}}{(\epsilon_l^m)^{\Theta_l^m}(1-\epsilon_l^m)^{1-\Theta_l^m}}\right\}^{-1}, \; l = 2, \cdots, L. \quad (4)$$

C. Opportunistic Channel Access

Let $D_m(t)$ be a decision variable for accessing channel m in time slot t. It is defined as

$$D_m(t) = \begin{cases} 0, & \text{if channel } m \text{ is considered idle} \\ 1, & \text{otherwise.} \end{cases} \quad (5)$$

We adopt a probabilistic approach: based on sensing results $\vec{\Theta}_m$, we have $D_m(t) = 0$ with probability $P_m^D(\vec{\Theta}_m)$ and $D_m(t) = 1$ with probability $1 - P_m^D(\vec{\Theta}_m)$.

For primary user protection, the collision probability with primary users due to CR user transmissions should be bounded below a threshold. Let γ_m be the maximum allowable collision probability with primary users on channel m. We have the following condition:

$$\left[1 - P_m^A(\vec{\Theta}_m)\right] P_m^D(\vec{\Theta}_m) \leq \gamma_m. \quad (6)$$

For CR network throughput performance, $P_m^D(\vec{\Theta}_m)$ should be set as large as possible. Since it is between 0 and 1, we have

$$P_m^D(\vec{\Theta}_m) = \min\left\{\gamma_m / \left[1 - P_m^A(\vec{\Theta}_m)\right], 1\right\}. \quad (7)$$

Let $\mathcal{A}(t) := \{m | D_m(t) = 0\}$ be the set of available channels in time slot t. Then $G^t = \sum_{m \in \mathcal{A}(t)} P_m^A(\Theta_1^m)$ is the expected number of available channels. These channels will be accessed in the transmission phase of this time slot.

D. Channel Fading Model

Without loss of generality, we consider independent block fading channels that is widely used in prior work [19]. The channel fading-gain process is piecewise constant on blocks of one time slot, and fading in different time slots are independent. Let $f_X^{i,j}(x)$ denote the *probability density function* of the received SINR X from a base station i (i.e.,

either an FBS or the MBS) at CR user j. We assume the packet can be successfully decoded if the received SINR exceeds a threshold H. The packet loss probability from base station i to CR user j is

$$P_{i,j}^F = \Pr\{X \le H\} = \int_0^H f_X^{i,j}(x)dx = F_X^{i,j}(H), \quad (8)$$

where $F_X^{i,j}(H)$ is the cumulative density function of X. If the packet is successfully decoded, the CR user returns an acknowledgment (ACK) to the base station in the ACK phase. We assume ACKs are always successfully delivered.

E. Video Performance Measure

We assume each active CR user receives a real-time video stream from either the MSB or an FSB. We adopt the MGS option of H.264/SVC, which can achieve better rate-distortion performance over MPEG-4 FGS [5], as well as providing scalability to accommodate the high variability of network bandwidth in CR networks. Due to real-time constraint, each Group of Pictures (GOP) of a video stream must be delivered in the next T time slots. Video packets are transmitted in the decreasing order of their significances in improving the quality of reconstructed video, with retransmissions if necessary. Overdue packets will be discarded.

Without loss of generality, we assume that the last wireless hop is the bottleneck; video data is available at the MBS and FBS's when they are scheduled to be transmitted. The quality of reconstructed MGS video can be modeled as [5]:

$$W(R) = \alpha + \beta \times R, \quad (9)$$

where $W(R)$ is the average peak signal-to-noise ratio (PSNR) of the reconstructed video, R is the received data rate, α and β are constants depending on the specific video sequence and codec. Note that $W(R)$ is average PSNR, which considers factors such as decoding dependencies and error propagations among received video frames.

IV. MGS Video over Femtocell CR Networks

A. Case of Single FBS

1) Formulation: We first consider the case of a single FBS in the CR network, where the FBS can use all the available channels to stream videos to K active CR users. Let w_j^t be the PSNR of CR user j at the beginning of time slot t and W_j^t the PSNR of CR user j at the end of time slot t. In time slot t, w_j^t is already known; W_j^t is a random variable that depends on channel condition and primary user activity; and w_j^{t+1} is a *realization* of W_j^t. Let $\xi_{0,j}^t$ and $\xi_{1,j}^t$ indicate the random packet losses from the MBS and FBS, respectively, to CR user j in time slot t. That is, $\xi_{i,j}^t$ is 1 with probability $\bar{P}_{i,j}^F(t) = 1 - P_{i,j}^F(t)$ and 0 with probability $P_{i,j}^F(t)$. Due to block fading channels, $P_{i,j}^F(t)$'s do not change within the time slot.

For *proportional fairness*, we aim to maximize the sum of the logarithms of received PSNRs of all CR users [20]. We formulate a *multistage stochastic programming problem* to maximize the expected logarithm-sum at time T.

$$\begin{aligned}
\text{maximize: } & \textstyle\sum_{j=1}^K \mathbb{E}[\log(W_j^T)] \quad (10)\\
\text{subject to: } & W_j^t = W_j^{t-1} + \xi_{0,j}^t \rho_{0,j}^t R_{0,j} + \xi_{1,j}^t \rho_{1,j}^t G^t R_{1,j},\\
& \qquad j = 1, \cdots, K,\ t = 1, \cdots, T\\
& \textstyle\sum_{j=1}^K \rho_{i,j}^t \le 1,\ \ i = 0, 1,\ t = 1, \cdots, T\\
& \rho_{i,j}^t \ge 0,\ i = 0, 1,\ j = 1, \cdots, K,\ t = 1, \cdots, T.
\end{aligned}$$

The optimization variables $\rho_{0,j}^t$ and $\rho_{1,j}^t$ are the portions of time slot t when CR user j receives video data from the MBS and FBS, respectively. Recall that G^t is the expected number of available channels in time slot t. $R_{0,j} = \beta_j B_0/T$ and $R_{1,j} = \beta_j B_1/T$ are constants for the j-th MGS video. Since OFDM is adopted, the total data rate is the number of available channels G^t times the bandwidth of each channel $R_{1,j}$, as in the first constraint.

When $t = 1$, W_j^0 is equal to α_j. At the beginning of the last time slot $t = T$, a realization $\boldsymbol{\xi}_{[T-1]} = [\boldsymbol{\xi}_1, \cdots, \boldsymbol{\xi}_{T-1}]$ is known, where $\boldsymbol{\xi}_t = [\xi_{0,1}^t, \cdots, \xi_{0,K}^t, \xi_{1,1}^t, \cdots, \xi_{1,K}^t]$, $t = 1, 2, \cdots, T-1$. It can be shown that the multistage stochastic programming problem (10) can be decomposed into T serial sub-problems, each to be solved in a time slot t [14].

$$\begin{aligned}
\text{maximize: } & \textstyle\sum_{j=1}^K \mathbb{E}\{\log(W_j^t)|\boldsymbol{\xi}_{[t-1]}\} \quad (11)\\
\text{subject to: } & W_j^t = W_j^{t-1} + \xi_{0,j}^t \rho_{0,j}^t R_{0,j} + \xi_{1,j}^t \rho_{1,j}^t G^t R_{1,j}\\
& \qquad j = 1, \cdots, K\\
& \textstyle\sum_{j=1}^K \rho_{i,j}^t \le 1,\ \ i = 0, 1\\
& \rho_{i,j}^t \ge 0,\ i = 0, 1,\ j = 1, \cdots, K,
\end{aligned}$$

where $\mathbb{E}\{\log(W_j^t)|\boldsymbol{\xi}_{[t-1]}\}$ denotes the *conditional expectation* of $\log(W_j^t)$ given realization $\boldsymbol{\xi}_{[t-1]}$. W_j^{t-1} is known given the realization. When $t = 1$, the conditional expectation becomes an unconditional expectation.

Since a CR user has only one transceiver, it can operate on either one or more licensed channels (i.e., connecting to the FBS) or the common channel (i.e., connecting to the MBS), but not both simultaneously. Assume CR user j operates on the common channel with probability p_j^t and one or more licensed channels with probability q_j^t. We then rewrite problem (11) as

$$\begin{aligned}
\text{maximize: } & \textstyle\sum_{j=1}^K \big[p_j^t \bar{P}_{0,j}^F(t) \log(W_j^{t-1} + \rho_{0,j}^t R_{0,j}) + \quad (12)\\
& \qquad q_j^t \bar{P}_{1,j}^F(t) \log(W_j^{t-1} + \rho_{1,j}^t G^t R_{1,j})\big]\\
\text{subject to: } & \textstyle\sum_{j=1}^K \rho_{i,j}^t \le 1,\ \ i = 0, 1\\
& p_j^t + q_j^t = 1,\ \ j = 1, \cdots, K\\
& \rho_{i,j}^t,\ p_j^t,\ q_j^t \ge 0,\ \ i = 0, 1,\ j = 1, \cdots, K.
\end{aligned}$$

2) Properties: We next analyze the formulated problem (12) and derive its properties. We have Lemmas 1, 2, and 3 and Theorem 1 and provide the proofs in the following.

Lemma 1: Prob. (12) is a convex optimization problem.

Proof: First, it can be shown that the single term $p_j^t \bar{P}_{0,j}^F(t)\log(W_j^{t-1}+\rho_{0,j}^t R_{0,j}) + q_j^t \bar{P}_{1,j}^F(t)\log(W_j^{t-1}+\rho_{1,j}^t G^t R_{1,j})$ is a concave function, because its *Hessian matrix* is negative semi-definite. Then, the objective function is concave since the sum of concave functions is also concave. Finally, all the constraints are linear. We conclude that problem (12) is convex since it is a maximization problem with a concave objective function and convex constraints. It has a unique optimal solution. ■

Lemma 2: If $[\rho^t, p^t, q^t]$ is a feasible solution to problem (12), then $[\rho^t, q^t, p^t]$ is also feasible.

Proof: Since $[\rho^t, p^t, q^t]$ is feasible, we have $p^t+q^t=1$. Switching the two probabilities, we still have $q^t+p^t=1$. Therefore, the derived new solution is also feasible. ■

Lemma 3: Let the optimal solution be $[\rho^{t*}, p^{t*}, q^{t*}]$. If $p_j^{t*} \geq q_j^{t*}$, then $\bar{P}_{0,j}^F(t)\log(W_j^{t-1}+\rho_{0,j}^{t*}R_{0,j})$ is greater than or equal to $\bar{P}_{1,j}^F(t)\log(W_j^{t-1}+\rho_{1,j}^{t*}G^t R_{1,j})$. And vice versa.

Proof: Assume $\bar{P}_{0,j}^F(t)\log(W_j^{t-1}+\rho_{0,j}^{t*}R_{0,j})$ is less than $\bar{P}_{1,j}^F(t)\log(W_j^{t-1}+\rho_{1,j}^{t*}G^t R_{1,j})$. Since $p_j^{t*} \geq q_j^{t*}$, the sum $p_j^{t*}\bar{P}_{0,j}^F(t)\log(W_j^{t-1}+\rho_{0,j}^{t*}R_{0,j}) + q_j^{t*}\bar{P}_{1,j}^F(t)\log(W_j^{t-1}+\rho_{1,j}^{t*}G^t R_{1,j})$ is smaller than the sum $q_j^{t*}\bar{P}_{0,j}^F(t)\log(W_j^{t-1}+\rho_{0,j}^{t*}R_{0,j}) + p_j^{t*}\bar{P}_{1,j}^F(t)\log(W_j^{t-1}+\rho_{1,j}^{t*}G^t R_{1,j})$. Thus we can obtain an objective value larger than the optimum by switching the values of p_j^{t*} and q_j^{t*}, which is still feasible according to Lemma 2. This conflicts with the assumption that $[\rho^{t*}, p^{t*}, q^{t*}]$ is optimal. The reverse statement can be proved similarly. ■

Theorem 1: Let the optimal solution be $[\rho^{t*}, p^{t*}, q^{t*}]$. If $p_j^{t*} > q_j^{t*}$, then we have $p_j^{t*}=1$ and $q_j^{t*}=0$. Otherwise, we have $p_j^{t*}=0$ and $q_j^{t*}=1$.

Proof: If $p_j^{t*} > q_j^{t*}$, we have $\bar{P}_{0,j}^F(t)\log(W_j^{t-1}+\rho_{0,j}^{t*}R_{0,j}) \geq \bar{P}_{1,j}^F(t)\log(W_j^{t-1}+\rho_{1,j}^{t*}G^t R_{1,j})$ according to Lemma 3. Since the objective function is linear with respect to p_j^t and q_j^t, the optimal value can be achieved by setting p_j^t to its maximum value 1 and q_j^t to its minimum value 0. The reverse statement can be proved similarly. ■

According to Theorem 1, a CR user is connected to either the MBS or the FBS for the *entire* duration of a time slot in the optimal solution. That is, it does not switch between base stations during a time slot under optimal scheduling.

3) Distributed Solution Algorithm: To solve problem (12), we define non-negative *dual variables* $\lambda=[\lambda_0,\lambda_1]$ for the inequality constraints. The *Lagrangian function* is

$$\begin{aligned}\mathcal{L}(p^t,\rho^t,\lambda) &= \textstyle\sum_{j=1}^K \big[p_j^t \bar{P}_{0,j}^F(t)\log(W_j^{t-1}+\rho_{0,j}^t R_{0,j}) + \\ &\quad (1-p_j^t)\bar{P}_{1,j}^F(t)\log(W_j^{t-1}+\rho_{1,j}^t G^t R_{1,j})\big] + \\ &\quad \lambda_0(1-\textstyle\sum_{j=1}^K \rho_{0,j}^t) + \lambda_1(1-\textstyle\sum_{j=1}^K \rho_{1,j}^t) \\ &= \textstyle\sum_{j=1}^K \mathcal{L}_j(p_j^t,\rho_{0,j}^t,\rho_{1,j}^t,\lambda_0,\lambda_1) + \lambda_0+\lambda_1 \quad (13)\end{aligned}$$

where $\mathcal{L}_j(p_j^t,\rho_{0,j}^t,\rho_{1,j}^t,\lambda_0,\lambda_1) = p_j^t\bar{P}_{0,j}^F(t)\log(W_j^{t-1}+\rho_{0,j}^t R_{0,j}) + (1-p_j^t)\bar{P}_{1,j}^F(t)\log(W_j^{t-1}+\rho_{1,j}^t G^t R_{1,j}) - \lambda_0\rho_{0,j}^t - \lambda_1\rho_{1,j}^t$.

The corresponding problem can be decomposed into K sub-problems and solved iteratively. In Step $\tau \geq 1$, for given $\lambda_0(\tau)$ and $\lambda_1(\tau)$ values, each CR user j solves the following sub-problem using local information.

$$\begin{aligned}&[p_j^{t*}(\tau),\rho_{0,j}^{t*}(\tau),\rho_{1,j}^{t*}(\tau)] \\ &= \underset{p_j^t,\rho_{0,j}^t,\rho_{1,j}^t \geq 0}{\arg\max}\ \mathcal{L}_j(p_j^t,\rho_{0,j}^t,\rho_{1,j}^t,\lambda_0(\tau),\lambda_1(\tau)). \quad (14)\end{aligned}$$

There is a unique optimal solution since the objective function in (14) is concave. The CR users then exchange their solutions. The *master dual problem*, for given $p^t(\tau)$ and $\rho^t(\tau)$, is:

$$\begin{aligned}&\min_{\lambda\geq 0} \mathcal{L}(p^t(\tau),\rho^t(\tau),\lambda) \\ &= \textstyle\sum_{j=1}^K \mathcal{L}_j(p_j^t(\tau),\rho_{0,j}^t(\tau),\rho_{1,j}^t(\tau),\lambda_0,\lambda_1) + \lambda_0+\lambda_1 \quad (15)\end{aligned}$$

Since the Lagrangian function is differentiable, the *gradient iteration* approach can be used.

$$\lambda_i(\tau+1) = \Big[\lambda_i(\tau) - s\times\Big(1-\textstyle\sum_{j=1}^K \rho_{i,j}^{t*}(\tau)\Big)\Big]^+, i=0,1, \quad (16)$$

where s is a sufficiently small positive *step size* and $[\cdot]^+$ denotes the projection onto the nonnegative axis. The updated $\lambda_i(\tau+1)$ will again be used to solve the sub-problems, and so forth. Since the problem is convex, we have *strong duality*; the *duality gap* between the primal and dual problems is zero. The dual variables $\lambda(\tau)$ will converge to the optimal values as τ goes to infinity. Since the optimal solution to (14) is unique, the primal variables $p^t(\tau)$ and $\rho_{i,j}^t(\tau)$ will also converge to their optimal values when τ is sufficiently large.

The resource allocation problem is jointly solved by the CR users and the MBS in the sensing phase of the time slot. For given λ_0 and λ_1, each CR user solves sub-problem (14) using local information. They then transmit their solutions $\rho_{i,j}^{t*}(\tau)$ to the MBS. The MBS will update the dual variables based on the received $\rho_{i,j}^{t*}(\tau)$'s as given in (16), and broadcast the updated λ_0 and λ_1 to all the CR users. This procedure is repeated iteratively until convergence.

The distributed solution procedure is presented in Table I. In the table, Steps 3–8 solve the sub-problem in (14); Step 9 updates the dual variables. The threshold ϕ is a prescribed small value with $0 \leq \phi \ll 1$. The algorithm terminates when the dual variables are sufficiently close to the optimal values.

B. Case of Multiple Non-interfering FBS's

We next consider the case of $N > 1$ non-interfering FBS's. The coverages of the FBS's do not overlap with each other, as FBS 1 and 2 in Fig. 1. Consequently, each FBS can use all the available licensed channels without interfering other FBS's. Assume each CR user knows the nearest FBS and is associate with it. Let $\mathcal{U}_i$ denote the set

Table I
ALGORITHM FOR THE CASE OF SINGLE FBS

Set $\tau = 0$, $\lambda_0(0)$ and $\lambda_1(0)$ to some nonnegative value
DO % (each CR user j executes Steps 3–8)
  $\rho_{0,j}^t(\tau) = \left[\frac{\bar{P}_{0,j}^F(t)}{\lambda_0(\tau)} - \frac{W_j^{t-1}}{R_{0,j}}\right]^+$ and
  $\rho_{1,j}^t(\tau) = \left[\frac{\bar{P}_{1,j}^F(t)}{\lambda_1(\tau)} - \frac{W_j^{t-1}}{R_{1,j}G^t}\right]^+$;
  IF $\left[\bar{P}_{0,j}^F(t)\log(W_j^{t-1} + \rho_{0,j}^t(\tau)R_{0,j}) - \lambda_0(\tau)\rho_{0,j}^t(\tau)\right] > \left[\bar{P}_{1,j}^F(t)\log(W_j^{t-1} + \rho_{1,j}^t(\tau)G^tR_{1,j}) - \lambda_1(\tau)\rho_{1,j}^t(\tau)\right]$
    Set $p_j^t(\tau) = 1$ and $\rho_{1,j}^t(\tau) = 0$;
  ELSE
    Set $p_j^t(\tau) = 0$ and $\rho_{0,j}^t(\tau) = 0$;
  END IF
  MBS updates $\lambda_i(\tau+1)$ as in (16);
  $\tau = \tau + 1$;
WHILE $\left(\sum_{i=0}^{1}(\lambda_i(\tau+1) - \lambda_i(\tau))^2 > \phi\right)$

of CR users associated with FBS i. The resource allocation problem becomes:

$$\begin{aligned}\text{maximize: } & \textstyle\sum_{j=1}^K p_j^t \bar{P}_{0,j}^F(t)\log(W_j^{t-1} + \rho_{0,j}^t R_{0,j}) + \\ & \textstyle\sum_{i=1}^N \sum_{j\in\mathcal{U}_i} q_j^t \bar{P}_{i,j}^F(t)\log(W_j^{t-1} + \rho_{i,j}^t G^t R_{i,j}) \\ \text{subject to: } & \textstyle\sum_{j=1}^K \rho_{0,j}^t \le 1 \\ & \textstyle\sum_{j\in\mathcal{U}_i}\rho_{i,j}^t \le 1, \;\; i = 1,\cdots,N \\ & p_j^t + q_j^t = 1, \;\; j = 1,\cdots,K \\ & \rho_{i,j}^t,\; p_j^t,\; q_j^t \ge 0, \;\; i = 1,\cdots,N,\; j = 1,\cdots,K.\end{aligned} \tag{17}$$

Since all the available channels can be allocated to each FBS simultaneously (i.e., with spatial reuse), problem (17) can be solved using the algorithm in Table I with some modified notation: $\rho_{1,j}^t(\tau)$ now becomes $\rho_{i,j}^t(\tau)$ and $\lambda_1(\tau)$ becomes $\lambda_i(\tau)$, $i = 1,\cdots,N$. The dual variables are iteratively updated as

$$\lambda_0(\tau+1) = \left[\lambda_0(\tau) - s\times\left(1 - \textstyle\sum_{j=1}^K \rho_{0,j}^{t*}(\tau)\right)\right]^+ \tag{18}$$

$$\lambda_i(\tau+1) = \left[\lambda_i(\tau) - s\times\left(1 - \textstyle\sum_{j\in\mathcal{U}_i}\rho_{i,j}^{t*}(\tau)\right)\right]^+, \quad i = 1,\cdots,N. \tag{19}$$

The modified solution algorithm is presented in Table II. As in the case of single FBS, the algorithm is jointly executed by the CR users and MBS, by iteratively updating the dual variables $\lambda_0(\tau)$ and $\lambda_i(\tau)$'s, and the resource allocations $\rho_{0,j}^{t*}(\tau)$ and $\rho_{i,j}^{t*}(\tau)$'s. It can be shown that the distributed algorithm can produce the optimal solution for problem (17).

C. Case of Multiple Interfering FBS's

1) Formulation: Finally, we consider the case of multiple interfering FBS's. Assume that the coverages of some FBS's overlap with each other, as FBS 3 and 4 in Fig. 1. They cannot use the same channel simultaneously, but have to compete for the channels during the transmission phase.

Table II
ALGORITHM FOR THE CASE OF MULTIPLE NON-INTERFERING FBS'S

Set $\tau = 0$, and $\lambda_0(0)$ and $\lambda_i(0)$ to some nonnegative values, for all i;
DO % (each CR user j executes Steps 3–8)
  $\rho_{0,j}^t(\tau) = \left[\frac{\bar{P}_{0,j}^F(t)}{\lambda_0(\tau)} - \frac{W_j^{t-1}}{R_{0,j}}\right]^+$ and
  $\rho_{i,j}^t(\tau) = \left[\frac{\bar{P}_{i,j}^F(t)}{\lambda_i(\tau)} - \frac{W_j^{t-1}}{R_{i,j}G^t}\right]^+$;
  IF $\left[\bar{P}_{0,j}^F(t)\log(W_j^{t-1} + \rho_{0,j}^t(\tau)R_{0,j}) - \lambda_0(\tau)\rho_{0,j}^t(\tau)\right] > \left[\bar{P}_{i,j}^F(t)\log(W_j^{t-1} + \rho_{i,j}^t(\tau)G^tR_{i,j}) - \lambda_i(\tau)\rho_{i,j}^t(\tau)\right]$
    Set $p_j^t(\tau) = 1$ and $\rho_{i,j}^t(\tau) = 0$;
  ELSE
    Set $p_j^t(\tau) = 0$ and $\rho_{0,j}^t(\tau) = 0$;
  END IF
  MBS updates $\lambda_i(\tau+1)$ as in (18) and (19);
  $\tau = \tau + 1$;
WHILE $\left(\sum_{i=0}^{N}(\lambda_i(\tau+1) - \lambda_i(\tau))^2 > \phi\right)$

Figure 2. Interference graph for the femtocell CR network shown in Fig. 1.

Define *channel allocation variables* $c_{i,m}^t$ for time slot t as:

$$c_{i,m}^t = \begin{cases} 1, & \text{if channel } m \text{ is allocated to FBS } i \\ 0, & \text{otherwise.}\end{cases} \tag{20}$$

Given an allocation, the expected number of available channels for FBS i is $G_i^t = \sum_{m\in\mathcal{A}(t)} c_{i,m}^t P_m^A$.

We use *interference graph* to model the case of overlapping coverages, which is defined below.

Definition 1: An *interference graph* $G_I = (V_I, E_I)$ is an undirected graph where each vertex represents an FBS and each edge indicates interference between the two end FBS's.

For the example network given in Fig. 1, we can derive an interference graph as shown in Fig. 2, with two isolated vertices FBS 1 and 2, and an edge connecting FBS 3 and 4. FBS 3 and 4 cannot use the same channel simultaneously, as summarized in the following lemma.

Lemma 4: If channel m is allocated to FBS i, the neighboring vertices of FBS i in the interference graph G_I, denoted as $\mathcal{R}(i)$, cannot use the same channel m simultaneously.

Further define index variables d_i^k, which is 1 if FBS i is an endpoint of link $k \in G_I$ and 0 otherwise, $i = 1,\cdots,N$. The interference constraint can be described as $\sum_{i=1}^N d_i^k c_{i,m}^t \le 1$, for $m = 0,\cdots,M$, and for all link $k \in G_I$. We then have the following problem formulation.

$$\begin{aligned}\text{maximize: } & \textstyle\sum_{j=1}^K p_j^t \bar{P}_{0,j}^F(t)\log(W_j^{t-1} + \rho_{0,j}^t R_{0,j}) + \\ & \textstyle\sum_{i=1}^N \sum_{j\in\mathcal{U}_i} q_j^t \bar{P}_{i,j}^F(t)\log(W_j^{t-1} + \rho_{i,j}^t G_i^t R_{i,j}) \\ \text{subject to: } & \textstyle\sum_{j=1}^K \rho_{0,j}^t \le 1 \\ & \textstyle\sum_{j\in\mathcal{U}_i}\rho_{i,j}^t \le 1, \;\; i = 1,\cdots,N \\ & p_j^t + q_j^t = 1, \;\; j = 1,\cdots,K\end{aligned} \tag{21}$$

Table III
ALGORITHM FOR CASE OF INTERFERING FBS'S

1:	Initialize $\boldsymbol{c}^t$ to a zero vector, FBS set $\mathcal{N} = \{1, \cdots, N\}$, and FBS-channel set $\mathcal{C} = \mathcal{N} \times \mathcal{A}(t)$;
2:	WHILE ($\mathcal{C}$ is not empty)
3:	Find FBS-channel pair $\{i', m'\}$, such that $\{i', m'\} = \arg\max_{\{i,m\}\in\mathcal{C}} \{Q(\boldsymbol{c}^t + \boldsymbol{e}_{i,m}) - Q(\boldsymbol{c}^t)\}$;
4:	Set $\boldsymbol{c}^t = \boldsymbol{c}^t + \boldsymbol{e}_{i',m'}$;
5:	Remove $\{i', m'\}$ from $\mathcal{C}$;
6:	Remove $\mathcal{R}(i') \times m'$ from $\mathcal{C}$;
7:	END WHILE

$$G_i^t = \sum_{m\in\mathcal{A}(t)} c_{i,m}^t P_m^A, \;\; i = 1, \cdots, N$$
$$\sum_{i=1}^N d_i^k c_{i,m}^t \leq 1, m = 0, \cdots, M, \text{for all link } k \in G_I,$$
$$\rho_{i,j}^t, p_j^t, q_j^t, c_{i,m}^t \geq 0,$$
$$i = 1, \cdots, N, \; j = 1, \cdots, K \; m = 0, \cdots, M,$$

2) Solution Algorithm : The optimal solution to problem (21) depends on the allocation variables $c_{i,m}^t$. Problem (21) can be solved with the algorithm in Table II if the $c_{i,m}^t$'s are known. Let $Q(\boldsymbol{c}^t)$ be the suboptimal objective value for a given channel allocation $\boldsymbol{c}^t$, where $\boldsymbol{c}^t = [\boldsymbol{c}_1^t, \boldsymbol{c}_2^t, \cdots, \boldsymbol{c}_N^t]$ and $\boldsymbol{c}_i^t$ is a vector of elements $c_{i,m}^t$, for FBS i and channel $m \in \mathcal{A}(t)$. If all the FBS's are disjointedly distributed with no overlap, each FBS can use all the available channels. We have $c_{i,m}^t = 1$ for all i and $m \in \mathcal{A}(t)$, i.e., it is reduced to the case in Section IV-B.

To solve problem (21), we first apply a *greedy algorithm* to allocate the available channels in $\mathcal{A}(t)$ to the FBS's (i.e., to determine $\boldsymbol{c}^t$). We then apply the algorithm in Table II to obtain a near-optimal solution. Let $\boldsymbol{e}_{i,m}$ be a unit vector with 1 at position $\{i, m\}$ (i.e., position $(i-1)\times M+m$) and 0 at all other positions, representing the allocation of channel $m \in \mathcal{A}(t)$ to FBS i. The greedy algorithm for channel allocation is presented in Table III, where the FBS-channel pair that can achieve the largest increase in the objective value $Q(\cdot)$ is chosen in each iteration. The worst case complexity of the greedy algorithm is $O(N^2M^2)$.

3) Performance Lower Bound: We next present a lower bound for the greedy algorithm. Let $e(l)$ be the l-th FBS-channel pair chosen in the greedy algorithm, and π_l the sequence $\{e(1), \cdots, e(l)\}$. The increase in object value (21) due to the l-th allocated FBS-channel pair is denoted as

$$\Delta_l := \Delta(\pi_l, \pi_{l-1}) = Q(\pi_l) - Q(\pi_{l-1}). \tag{22}$$

Since $Q(\pi_0) = Q(\emptyset) = 0$, we have

$$\begin{aligned}\sum_{l=1}^L \Delta_l &= Q(\pi_L) - Q(\pi_{L-1}) + \cdots + \\ &\quad Q(\pi_2) - Q(\pi_1) + Q(\pi_1) - Q(\pi_0) \\ &= Q(\pi_L) - Q(\pi_0) = Q(\pi_L).\end{aligned}$$

For two FBS-channel pairs $e(l)$ and $e(l')$, we say $e(l)$ *conflicts with* $e(l')$ when there is an edge connecting the FBS in $e(l)$ and the FBS in $e(l')$ in the interference graph G_I, and the two FBS's choose the same channel. Let Ω be the global optimal solution. We define ω_l as the subset of Ω that conflicts with allocation $e(l)$ but not with the previous allocations $\{e(1), e(2), \cdots, e(l-1)\}$.

Lemma 5: Assume the greedy algorithm in Table III stops in L steps. The global optimal solution Ω can be partitioned into L non-overlapping subsets ω_l, $l = 1, 2, \cdots, L$.

Proof: According to the definition of ω_l, the L subsets of the optimal solution Ω do not intersect with each other. Assume the statement is false, then the union of these L subsets is not equal to the optimal set Ω. Let the *set difference* be $\omega_{L+1} = \Omega \backslash (\cup_{l=1}^L \omega_l)$. By definition, ω_{L+1} does not conflict with the existing L allocations $\{e(1), \cdots, e(L)\}$, meaning that the greedy algorithm can continue to at least the $(L+1)$-th step. This conflicts with the assumption that the greedy algorithm stops in L steps. It follows that $\Omega = \cup_{l=1}^L \omega_l$. ■

Let $\Delta(\pi_2, \pi_1) = Q(\pi_2) - Q(\pi_1)$ denote the difference between two feasible allocations π_1 and π_2. We next derive a lower bound on the performance of the greedy algorithm. We assume two properties for function $\Delta(\pi_2, \pi_1)$.

Property 1: Consider FBS-channel pair sets π_1, π_2, and σ, satisfying $\pi_1 \subseteq \pi_2$ and $\sigma \cap \pi_2 = \emptyset$. We have $\Delta(\pi_2 \cup \sigma, \pi_1 \cup \sigma) \leq \Delta(\pi_2, \pi_1)$.

Property 2: Consider FBS-channel pair sets π, σ_1, and σ_2 satisfying $\sigma_1 \cap \pi = \emptyset$, $\sigma_2 \cap \pi = \emptyset$, and $\sigma_1 \cap \sigma_2 = \emptyset$. We have $\Delta(\sigma_1 \cup \sigma_2 \cup \pi, \pi) \leq \Delta(\sigma_1 \cup \pi, \pi) + \Delta(\sigma_2 \cup \pi, \pi)$.

In Property 1, we have $\sigma \cap \pi_1 = \emptyset$ since $\pi_1 \subseteq \pi_2$ and $\sigma \cap \pi_2 = \emptyset$. This property states that the incremental objective value does not get larger as more channels are allocated and as the objective value gets larger. Property 2 states that the incremental objective value achieved by allocating multiple FBS-channel pair sets does not exceed the sum of the incremental objective values achieved by allocating each individual FBS-channel pair set. These are generally true for many resource allocation problems [20].

Since we choose the maximum incremental allocation in each step of the greedy algorithm, we have Lemma 6 that directly follows Step 3 in Table III.

Lemma 6: For any FBS-channel pair $\sigma \in \omega_l$, we have $Q(\pi_{l-1} \cup \sigma) - Q(\pi_{l-1}) = \Delta(\pi_{l-1} \cup \sigma, \pi_{l-1}) \leq \Delta_l$.

Lemma 7: Assume the greedy algorithm stops in L steps, we have $Q(\Omega) \leq Q(\pi_L) + \sum_{l=1}^L \sum_{\sigma\in\omega_l} \Delta(\sigma \cup \pi_{l-1}, \pi_{l-1})$.

Proof: The following inequalities hold true according to the properties of the $\Delta(\cdot, \cdot)$ function:

$$\begin{aligned}&Q((\cup_{i=l+1}^L \omega_i) \cup \pi_l) = Q((\cup_{i=l+2}^L \omega_i) \cup \pi_l) \; + \\ &\qquad \Delta((\cup_{i=l+1}^L \omega_i) \cup \pi_l, (\cup_{i=l+2}^L \omega_i) \cup \pi_l) \\ &\leq Q((\cup_{i=l+2}^L \omega_i) \cup \pi_l) + \Delta(\omega_{l+1} \cup \pi_l, \pi_l) \\ &\leq Q((\cup_{i=l+2}^L \omega_i) \cup \pi_{l+1}) + \Delta(\omega_{l+1} \cup \pi_l, \pi_l) \\ &\leq Q((\cup_{i=l+2}^L \omega_i) \cup \pi_{l+1}) + \textstyle\sum_{\sigma\in\omega_{l+1}} \Delta(\sigma \cup \pi_l, \pi_l).\end{aligned}$$

We have $\pi_0 = \emptyset$ and $\omega_{L+1} = \emptyset$ (see Lemma 5). By induction from $l = 0$ to $l = L-1$, we have $Q((\cup_{i=1}^L \omega_i) \cup \emptyset) = Q(\Omega)$

and $Q(\Omega) \leq Q(\pi_L) + \sum_{l=1}^{L} \sum_{\sigma \in \omega_l} \Delta(\sigma \cup \pi_{l-1}, \pi_{l-1})$. ■

Lemma 8: The maximum size of ω_l is equal to the degree, in the interference graph G_I, of the FBS selected in the l-th step of the greedy algorithm, which is denoted as $D(l)$.

Proof: Once FBS i is allocated with channel m, the neighboring FBS's in G_I, $\mathcal{R}(i)$, cannot use the same channel m anymore due to the interference constraint. The maximum number of FBS-channel pairs that conflict with the selected FBS-channel pair $\{i, m\}$, i.e., the maximum size of ω_l, is equal to the degree of FBS i in G_I. ■

Theorem 2: The greedy algorithm can achieve an objective value that is at least $\frac{1}{1+D_{max}}$ of the global optimum, where D_{max} is the maximum node degree in the interference graph G_I of the femtocell CR network.

Proof: According to Lemmas 7 and 8, we have:

$$Q(\Omega) \leq Q(\pi_L) + \sum_{l=1}^{L} D(l)\Delta_l = Q(\pi_L) + \bar{D}\sum_{l=1}^{L}\Delta_l = (1+\bar{D})Q(\pi_L), \quad (23)$$

where $\bar{D} = \sum_{l=1}^{L} D(l)\Delta_l / \sum_{l=1}^{L} \Delta_l$. The second equality is due to the facts that $\Delta_l = Q(\pi_l) - Q(\pi_{l-1})$ and $\sum_{l=1}^{L} \Delta_l = Q(\pi_L)$. To further simplify the bound, we replace $D(l)$ with the maximum node degree D_{max}. It follows that $\bar{D} \leq \sum_{l=1}^{L} D_{max}\Delta_l / \sum_{l=1}^{L} \Delta_l = D_{max}$ and

$$\frac{1}{1+D_{max}} Q(\Omega) \leq Q(\pi_L) \leq Q(\Omega), \quad (24)$$

which provides a lower bound on the performance of the greedy algorithm. ■

When there is a single FBS in the CR network, we have $D_{max} = 0$ and $Q(\pi_L) = Q(\Omega)$ according to Theorem 2. The proposed algorithm produces the optimal solution. In the case of multiple non-interfering FBS's, we still have $D_{max} = 0$ and can obtain the optimal solution using the proposed algorithm. For the femtocell CR network given in Fig. 1 (with interference graph shown in Fig. 2), we have $D_{max} = 1$ and the low bound is a half of the global optimal. Note that (23) provides a tighter bound for the optimum than (24), but with higher complexity. These are interesting performance bounds since they bound the achievable video quality, an application layer performance measure, rather than lower layer ones (e.g., bandwidth or time share).

V. Simulation Results

We evaluate the performance of the proposed algorithms using MATLAB and JVSM 9.13 Video Codec. Two scenarios are used in the simulations: a single FBS CR network and a CR network with interfering FBS's. In every simulation, we compare the proposed algorithms with the following two more straightforward heuristic schemes:

- Heuristic 1 based on *equal allocation*: each CR user chooses the better channel (i.e., the common channel or a licensed channel) based on the channel conditions; time slots are equally allocated among active CR users;

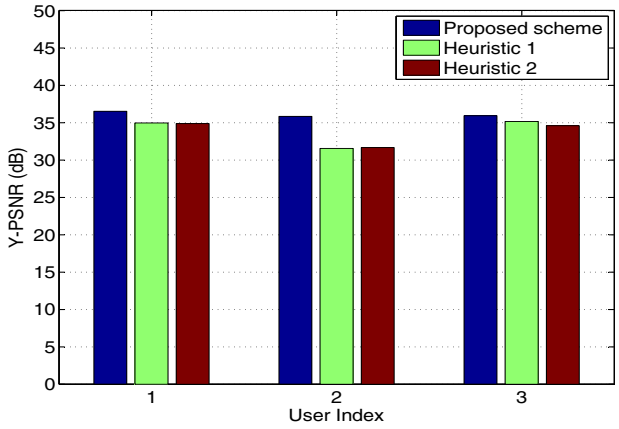

Figure 3. Single FBS: received video quality for the three CR users.

- Heuristic 2 exploiting *multiuser diversity*: the MBS and each FBS chooses one active CR user with the best channel condition; the entire time slot is allocated to the selected CR user.

Each point in the figures presented in this section is the average of 10 simulation runs. We also plot 95% confidence intervals in the figures, which are generally negligible.

A. Case of Single FBS

In the first scenario, there are $M = 8$ channels and the channel parameters P_{01}^m and P_{10}^m are set to 0.4 and 0.3, respectively, for all m. The maximum allowable collision probability γ_m is set to 0.2 for all m. There is one FBS and three active CR users. Three Common Intermediate Format (CIF, 352×288) video sequences are streamed to the CR users, i.e., *Bus* to CR user 1, *Mobile* to CR user 2, and *Harbor* to CR user 3. The GOP size of each video sequence is 16. The delivery deadline is $T = 10$. Both probabilities of false alarm ϵ and miss detection δ are set to 0.3 for all the FBS's and CR users, unless otherwise specified.

We first plot the average PSNRs of the three CR users in Fig. 3. Our proposed scheme achieves the best performance among the three algorithms, with up to 4.3 dB improvement over the two heuristic schemes. Such gains are significant with regard to video quality, since a 0.5 dB difference is distinguishable by human eyes. Compared to the two heuristic schemes, the video quality of our proposed scheme is well balanced among the three users, indicating better fairness performance for the CR users.

We next investigate the convergence of the distributed algorithm. The traces of the two dual variables are plotted in Fig. 4(a). Both dual variables converge to their optimal values after 500 iterations. After convergence, the optimal solution for the primary problem can be obtained.

In Fig. 4(b), we examine the impact of the number of channels M on received video quality. We increase M from 4 to 12 with step size 2, and plot the average PSNR values of the three received videos. As expected, the more licensed

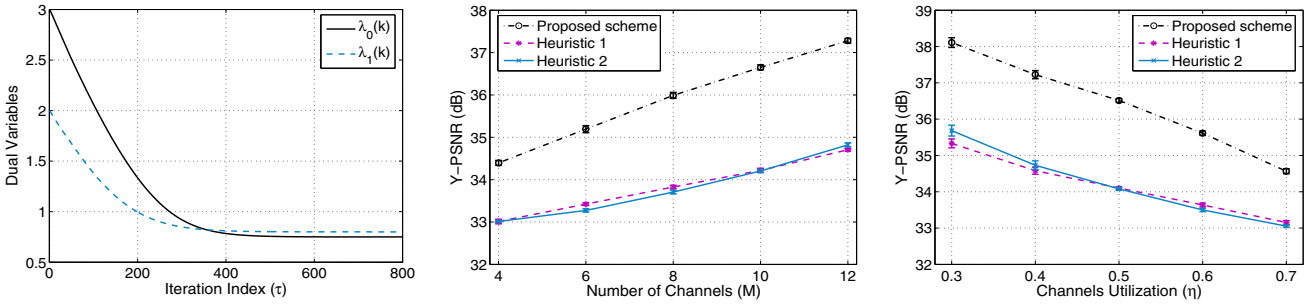

(a) Convergence of the two dual variables (b) Video quality vs. number of channels (c) Video quality vs. channel utilization

Figure 4. Simulation results for the Single FBS case.

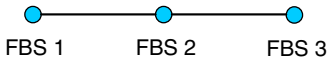

Figure 5. Interference graph for the network used in the simulation.

channels, the more spectrum opportunities for CR users and the higher PSNR for received video sequence. Both curves of heuristics 1 and 2 have lower slops than that of the proposed algorithm, implying that the proposed scheme is more efficient in exploiting the additional spectrum opportunities for video transmissions.

In Fig. 4(c), we demonstrate the impact of channel utilization η on received video quality. The average PSNRs are plotted when η is increased from 0.3 to 0.7. Intuitively, a smaller η allows more spectrum opportunities for video transmission. This is illustrated in the figure where all the three curves decrease as η gets larger. The performance of both heuristics are close and the proposed scheme achieves a gain about 3 dB over the heuristics.

B. Case of Interfering FBS's

We next investigate the second scenario with three FBS's, and each FBS has three active CR users. Each FBS streams three different videos to the corresponding CR users. The coverages of FBS 1 and 2 overlap with each other; the coverages of FBS 2 and 3 overlap with each other; however the coverages of FBS 1 and 3 do not overlap. The corresponding interference graph is shown in Fig. 5.

In Fig. 6(a), we investigate the impact of channel utilization η on the video quality. We increase η from 0.3 to 0.7 with step size 0.1, and plot the average PSNRs of all CR users achieved by the three schemes. A lower channel utilization provides more spectrum opportunities. The performance of the proposed scheme is the best among the three schemes. The reason why heuristic 2 achieves better performance than heuristic 1 is that the resource allocation decision is made globally in heuristic 2 but locally in heuristic 1. In heuristic 1, each CR user chooses a channel mode by itself regardless of other CR users. In heuristic 2, the allocation is made by the MBS and FBS's and the CR users with the best channel conditions are chosen. We also plot an upper bound on the optimal objective value, which is obtained as in (23). Note that this bound is tighter than that given in Theorem 2. We observe that the upper bound is about 0.4 dB higher than our proposed scheme, indicating that the gap between the results produced by the proposed scheme and the global optimal is less than 0.4 dB.

Next, we examine the impact of sensing errors on the received video quality. In Fig. 6(b), we test five pairs of $\{\epsilon, \delta\}$ values: $\{0.2, 0.48\}$, $\{0.24, 0.38\}$, $\{0.3, 0.3\}$, $\{0.38, 0.24\}$, and $\{0.48, 0.2\}$. The average PSNRs of all active CR users are plotted. It is interesting to see that the performance of all the three schemes get worse when the probability of one of the two sensing errors gets large. We can trade-off between false alarm and miss detection probabilities to find the optimal operating point for the spectrum sensors. On the other hand, the dynamic range of video quality is not big for the range of sensing errors simulated, compared to that in Fig. 6(a). This is because both sensing errors are modeled and treated in the algorithms. Again, our proposed scheme outperforms the two heuristic schemes with considerable margins for the entire range.

Finally, we investigate the impact of the bandwidth of the common channel B_0. In this simulation, we fix B_1 at 0.3 Mbps and increase B_0 from 0.1 Mbps to 0.5 Mbps with step size 0.1 Mbps. The results are presented in Fig. 6(c). We notice that the average video quality increases rapidly as the common channel bandwidth is increased from 0.1 Mbps to 0.3 Mbps. Beyond 0.3 Mbps, the increases of the PSNR curves slow down and the curves get flat. This implies that a very large bandwidth for the common channel is not necessary, since the gain for additional bandwidth diminishes as B_0 gets large. Again, we find our proposed scheme outperforms the other two heuristics and the gap between our scheme and the upper bound is small.

VI. Conclusion

In this paper, we investigated the problem of streaming multiple MGS videos in a femtocell CR network. We formulated a multistage stochastic programming problem

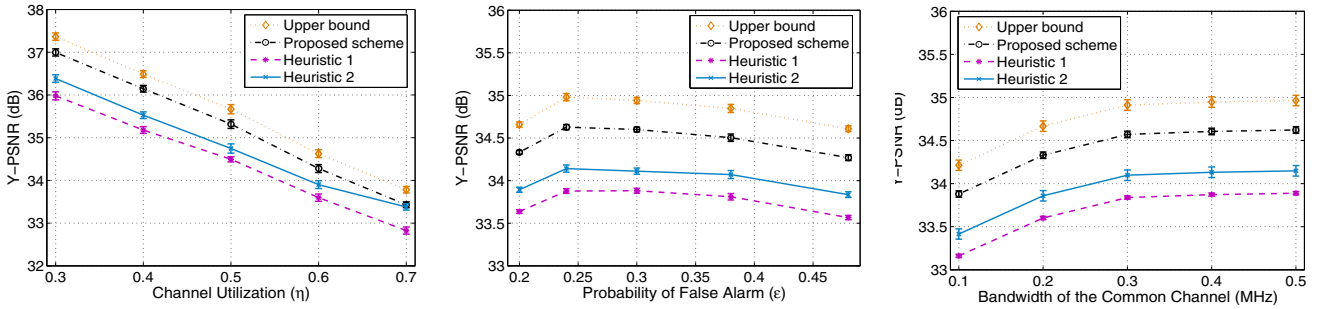

(a) Video quality vs. channel utilizations (b) Video quality vs. sensing error (c) Video quality vs. common channel bandwidth

Figure 6. Simulation results for the case of multiple interfering FBS's.

considering various design factors across multiple layers. We developed a solution algorithm that can produce the optimal solution in the case of non-interfering FBS's and a greedy algorithm for near-optimal solutions in the case of interfering FBS's. We also prove a lower bound for the greedy algorithm. The proposed algorithms are evaluated via simulations and are shown to outperform two alternative schemes with considerable gains.

ACKNOWLEDGMENT

This work is supported in part by the US National Science Foundation (NSF) under Grants CNS-0953513, ECCS-0802113, and IIP-1032002, and through the NSF Wireless Internet Center for Advanced Technology (WICAT) at Auburn University.

REFERENCES

[1] Cisco, "Visual Networking Index (VNI)," July 2010. [Online]. Available: http://www.cisco.com/

[2] V. Chandrasekhar, J. G. Andrews, and A. Gatherer, "Femtocell networks: a survey," *IEEE Commun. Mag.*, vol. 46, no. 9, pp. 59–67, Sept. 2008.

[3] R. Kim, J. S. Kwak, and K. Etemad, "WiMAX femtocell: requirements, challenges, and solutions," *IEEE Commun. Mag.*, vol. 47, no. 9, pp. 84–91, Sept. 2009.

[4] Q. Zhao and B. Sadler, "A survey of dynamic spectrum access," *IEEE Signal Process. Mag.*, vol. 24, no. 3, pp. 79–89, May 2007.

[5] M. Wien, H. Schwarz, and T. Oelbaum, "Performance analysis of SVC," *IEEE Trans. Circuits Syst. Video Technol.*, vol. 17, no. 9, pp. 1194–1203, Sept. 2007.

[6] V. Chandrasekhar, J. G. Andrews, T. Muharemovic, Z. Shen, and A. Gatherer, "Power control in two-tier femtocell networks," *IEEE Trans. Wireless Commun.*, vol. 8, no. 8, pp. 4316–4328, Aug. 2009.

[7] H.-C. Lee, D.-C. Oh, and Y.-H. Lee, "Mitigation of inter-femtocell interference with adaptive fractional frequency reuse," in *Proc. IEEE ICC 2010*, Cape Town, South Africa, May 2010, pp. 1–5.

[8] T. Alade, H. Zhu, and J. Wang, "Uplink co-channel interference analysis and cancellation in femtocell based distributed antenna system," in *Proc. IEEE ICC 2010*, Cape Town, South Africa, May 2010, pp. 1–5.

[9] Y. Zhao, S. Mao, J. Neel, and J. H. Reed, "Performance evaluation of cognitive radios: metrics, utility functions, and methodologies," *Proc. IEEE*, vol. 97, no. 4, pp. 642–659, Apr. 2009.

[10] J. Jin and B. Li, "Cooperative resource management in cognitive WiMAX with femto cells," in *Proc. IEEE INFOCOM 2010*, San Diego, CA, Mar. 2010, pp. 552–560.

[11] H.-P. Shiang and M. van der Schaar, "Dynamic channel selection for multi-user video streaming over cognitive radio networks," in *Proc. IEEE ICIP'08*, San Diego, CA, Oct. 2008, pp. 2316–2319.

[12] S. Ali and F. Yu, "Cross-layer QoS provisioning for multimedia transmissions in cognitive radio networks," in *Proc. IEEE WCNC'09*, Budapest, Hungary, Apr. 2009, pp. 1–5.

[13] L. Ding, S. Pudlewski, T. Melodia, S. Batalama, J. Matyjas, and M. Medley, "Distributed spectrum sharing for video streaming in cognitive radio ad hoc networks," in *Intl. Workshop on Cross-layer Design in Wireless Mobile Ad Hoc Networks*, Niagara Falls, Canada, Sept. 2009, pp. 1–13.

[14] D. Hu and S. Mao, "Streaming scalable videos over multi-hop cognitive radio networks," *IEEE Trans. Wireless Commun.*, vol. 9, no. 11, pp. 3501–3511, Nov. 2010.

[15] D. Hu, S. Mao, Y. Hou, and J. Reed, "Fine grained scalability video multicast in cognitive radio networks," *IEEE J. Sel. Areas Commun.*, vol. 28, no. 3, pp. 334–344, Apr. 2010.

[16] A. Motamedi and A. Bahai, "MAC protocol design for spectrum-agile wireless networks: stochastic control approach," in *Proc. IEEE DySPAN'07*, Dublin, Ireland, Apr. 2007, pp. 448–451.

[17] S. Geirhofer, L. Tong, and B. Sadler, "Cognitive medium access: constraining interference based on experimental models," *IEEE J. Sel. Areas Commun.*, vol. 26, no. 1, pp. 95–105, Jan. 2008.

[18] H. Su and X. Zhang, "Cross-layer based opportunistic MAC protocols for QoS provisionings over cognitive radio mobile wireless networks," *IEEE J. Sel. Areas Commun.*, vol. 26, no. 1, pp. 118–129, Jan. 2008.

[19] T. Rappaport, *Wireless Communications: Principles & Practice*, 2nd ed. Indianapolis, IN: Prentice Hall PTR, 2001.

[20] F. Kelly, A. Maulloo, and D. Tan, "Rate control in communication networks: shadow prices, proportional fairness and stability," *J. Oper. Res. Soc.*, vol. 49, no. 3, pp. 237–252, Mar. 1998.